Optimization of tin dioxide nanosticks faceting for the improvement of palladium nanocluster epitaxy

J. Arbiol,[a] A. Cirera, F. Peiró, A. Cornet, and J. R. Morante
EME Enginyeria i Materials Electrònics, Departament d'Electrònica, Universitat de Barcelona, E-08028 Barcelona, Spain

J. J. Delgado and J. J. Calvino
Departamento de Ciencia de los Materiales, Ingeniería Metalúrgica y Química Inorgánica, Universidad de Cádiz, Facultad de Ciencias, Puerto Real (Cádiz) E-11510, Spain

(Received 13 June 2001; accepted for publication 19 November 2001)

Semispherical palladium nanoclusters have been epitaxed on {110} facets of tin dioxide nanosticks. The synthesis of tin dioxide nanoparticles has been optimized to obtain a crystallite shape with a maximum surface area lying on the rutile structure {110} planes, which are the most active for gas sensing. For this purpose, we describe a microwave method, which allowed us to obtain monocrystalline stick-like tin dioxide nanoparticles (so-called nanosticks) with rectangular prism shape. These nanosticks present long lateral {110} faces, squared cross-section 5–25 nm wide, and lengths of up to 0.5 μm. © *2002 American Institute of Physics.* [DOI: 10.1063/1.1433903]

Since Seiyama *et al.*[1] introduced the possibility to use chemical sensors for gas sensing, several studies have focused on sensing materials; which exhibit changes of conductivity at gas exposure. Currently, SnO_2 is the most frequently used material in these semiconductor gas sensor (SGS) devices.[2,3] Semiconductor sensing material in a nanoparticle microstructure improves the response (sensitivity) of the SGS.[4] Moreover, it is known that the introduction of noble metals, such as platinum and palladium, improves SGS selectivity and decreases its operating temperatures.[5] Furthermore, both sensitivity and selectivity also depend on the distribution, chemical state, and crystal size of the noble metals added.[6]

In the last few years, much attention has been given to wirelike structures because of their low cross-section dimensionality in comparison with length, thereby promoting unidirectional space-confined carrier transport, which is of interest for multiple applications.[7] In a recent study, Pan *et al.*[8] synthesized ultralong belt-like nanostructures (so-called nanobelts) of undoped semiconducting oxides, such as tin dioxide or indium oxide, and proposed that the doping of these wirelike nanostructures with different elements could be used for making nanosized sensors on the basis of their unidirectional carrier transport characteristics.

In this letter, we present results on the effects of Pd as a catalytic additive to SnO_2 nanopowders. We also show that reduction treatments of Pd-loaded nanopowders greatly affect grain growth, promoting the formation of stick-like SnO_2 nanoparticles with wirelike structures.

The samples were synthesized by means of the microwave method, as reported in Ref. 2. In these previous studies, the low Pd loading (up to 3 at. Pd/Sn %) used during sample growth, allowed us to obtain SnO_2 nanopowders with quasispherical nanoparticles and a high dispersion of catalysts. As reported previously,[9] few nanosticks appeared among the spherical nanoparticles when the Pd load was increased (10 at. Pd/Sn %). In this study, spectacular results were obtained when samples were submitted to a reducing treatment. Reduction consisted of the following steps: (1) heating the Pd/SnO_2 sample in a flow of 5% H_2/Ar gas mixture (60 cm^3/min) at 10 K min^{-1} from room temperature (298 K) up to the selected reduction temperature (473 K). Samples were held for 2 h at the reduction temperature; (2) treatment in flowing helium (60 cm^3/min) for 1 h at the reduction temperature to remove adsorbed hydrogen; (3) cooling in flow of inert gas. To prevent the fast and uncontrolled reoxidation of the reduced samples, they were cooled to 191 K and then treated at low temperature with O_2 (5%)-He for 30 min, warmed to 295 K in the oxidizing mixture, and finally exposed to air. Further information about the reduction treatment can be found elsewhere.[10]

After this process we obtained stick-like tin dioxide nanoparticles (so-called nanosticks) (Fig. 1). These nanosticks presented typical widths in the range 5–25 nm, and lengths up to 0.5 μm. Moreover, metallic Pd particles, in the nanometer size range, were dispersed over the surface of these sticks (Fig. 1). The stick-like nanoparticles were monocrystalline, structurally uniform, and free of defects and dislocations, as observed by high resolution transmission

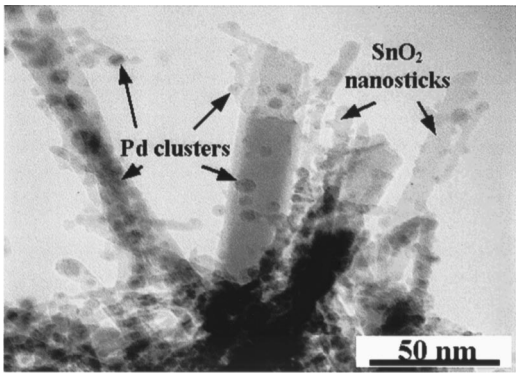

FIG. 1. Low magnification TEM image showing a general view of the SnO_2 nanosticks covered with Pd nanoclusters (in dark contrast).

[a]Electronic mail: arbiol@el.ub.es

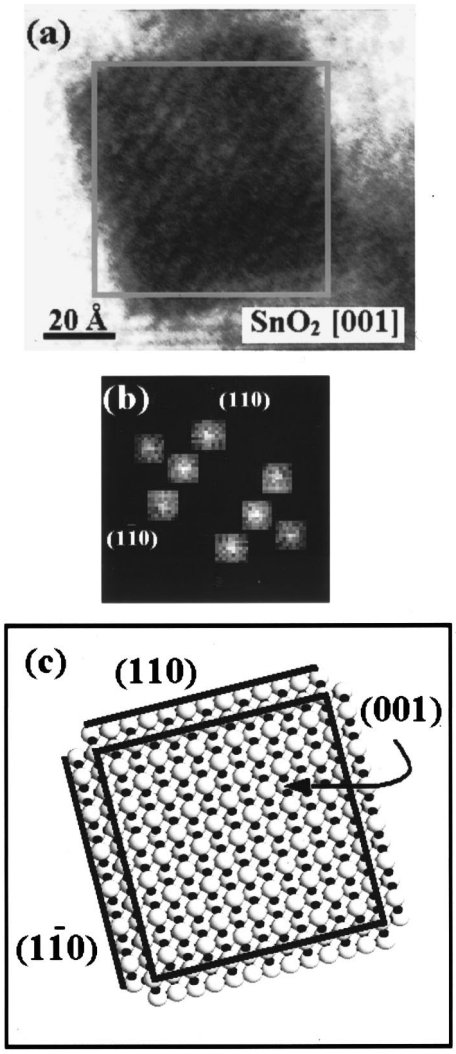

FIG. 2. (a) HRTEM micrograph corresponding to a SnO_2 nanostick cross section visualized in the [001] crystal direction; (b) digital diffraction pattern of the region squared in the top image; (c) nanostick model oriented along the [001] direction.

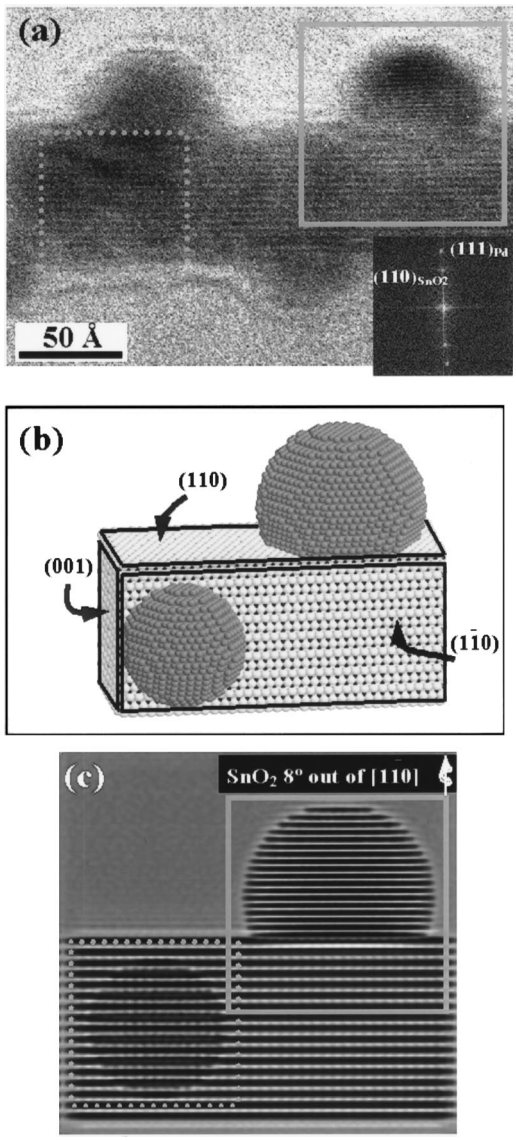

FIG. 3. (a) HRTEM micrograph showing Pd nanoclusters epitaxed on the surface of a SnO_2 nanostick both in profile view (e.g., selected in a solid square) and plan view (e.g., selected in dashed square). The inset shows the digital diffraction pattern of the solid square selection in (a); (b) supercell model of the Pd/SnO_2 epitaxial system; (c) computer image simulation of the model proposed in the middle.

electron microscopy (HRTEM). These nanoparticles had squared cross sections with rectangular prism shape and with long lateral faces corresponding to {110} planes, as seen after HRTEM analysis of the cross sections (Fig. 2). Pd nanoclusters are epitaxed on {110} SnO_2 surfaces. Epitaxial planes were determined from the details of HRTEM profile view images, and are shown in the solid black line squared selection in Fig. 3(a). We observed that $(111)_{Pd}$ planes grew parallel to $(110)_{SnO_2}$ reduced planes. For this interfacial relation, we tested an epitaxial model: $[1\text{-}10](111)_{Pd}\|[001](110)_{SnO_2}$ (Fig. 4). The atomic radii used to plot this figure were changed to allow observation of the atomic projections along the unit cell axis. Taking $(11\text{-}2)_{Pd}$ and $(1\text{-}10)_{SnO_2}$ planes as reference in the interface, we observed the following epitaxial relationship: twice the distance between $(11\text{-}2)_{Pd}$ planes is about the distance between the $(1\text{-}10)_{SnO_2}$ planes. The lateral misfit between these was -5.4%, $2\cdot d(11\text{-}2)_{Pd}=2\times 1.587$ Å $=3.174$ Å, and $d(1\text{-}10)_{SnO_2}=3.35$ Å. Moreover, if we consider $(1\text{-}10)_{Pd}$ and $(002)_{SnO_2}$ planes, a new coincidence relationship appears. In this case, in every three $(1\text{-}10)_{Pd}$ plane spacings a

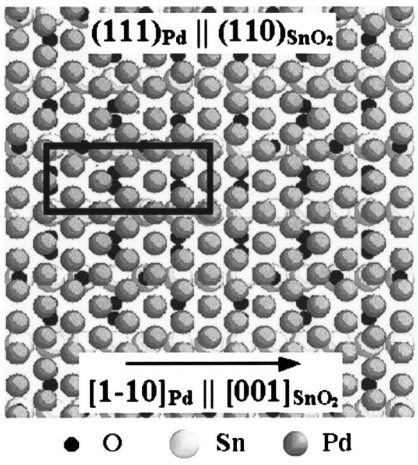

FIG. 4. Epitaxial model shown in plan view. The epitaxial relationship proposed is $[1\text{-}10](111)_{Pd}\|[001](110)_{SnO_2}$.

Pd atom coincides with a Sn atom in five $(002)_{SnO_2}$ plane spacings, giving an equivalent misfit of 3.4%; $3 \cdot d(1\text{-}10)_{Pd} = 3 \times 2.75\ \text{Å} = 8.25\ \text{Å}$; $5 \cdot d(002)_{SnO_2} = 5 \times 1.595\ \text{Å} = 7.975\ \text{Å}$. According to this structural correlation, we can define a small-size coincidence cell that is repeated periodically along the $[11\text{-}2]_{Pd}$ and $[1\text{-}10]_{Pd}$ directions. This coincidence cell, with dimensions $2 \cdot [11\text{-}2]_{Pd} \times 3 \cdot [1\text{-}10]_{Pd}$, is marked in Fig. 4.

To confirm our predictions about the epitaxial relationship, we also used the information obtained from plan view images. In this case we observed how $(\text{-}1\text{-}11)_{Pd}$ planes were aligned with $(1\text{-}10)_{SnO_2}$ planes. Taking into account the stereographic projection along the $[111]_{Pd}$ and $[110]_{SnO_2}$ directions, we found that the $(\text{-}1\text{-}11)_{Pd}$ plane projection was aligned with that of the $(\text{-}1\text{-}12)_{Pd}$ and therefore was aligned with $(1\text{-}10)_{SnO_2}$. These results indicate that our proposed epitaxial model was in good agreement with the experimental results. The epitaxial relationship proposed was modeled [Fig. 3(b)] using the program RHODIUS.[11] Computer image simulation of the model was done with the software package EMS,[12] [Fig. 3(c)]. The good match between experimental and calculated images confirms that Pd nanoclusters adopt semispherical shape and that they grow epitaxed on SnO_2 stick-like particles after reduction.

Moreover, the presence of high Pd loading has a strong effect on the SnO_2 growing mode, thereby determining the faceting of the rutile nanoparticles in the faces observed during the growth steps. This effect was demonstrated by comparing the shape of these stick-like nanoparticles obtained at high Pd loadings with that observed for SnO_2 nanopowders obtained at low loadings, where SnO_2 nanoparticles had quasispherical shapes and nanosticks were not present.[2] Likewise, the reduction process is shown to enhance the effect of Pd over the shape of SnO_2 nanoparticles. While only few SnO_2 nanoparticles adopted the nanostick shape before reduction, almost all of them acquired the desired stick-like nanostructure after this process.

In this letter we also report on the distribution of the metal loading in these special nanostructures. Growth conditions and treatments were optimized to obtain epitaxial growth between metal nanoclusters and nanosticks {110} facets. We are currently working on the electrical characterization of the response of these nanosticks to gases.

This work was partially funded by the EU INCO Project No. ICA2-CT-2000-10017 and by the Spanish CICYT Program No. MAT 99-0435-C02-01.

[1] T. Seiyama, A. Kato, K. Fujisishi, and M. Nagatoni, Anal. Chem. **34**, 1052 (1962).
[2] A. Cirera, A. Vilà, A. Diéguez, A. Cabot, A. Cornet, and J. R. Morante, Sens. Actuators B **64**, 65 (2000).
[3] K. Sekizawa, H. Widjaja, S. Maeda, Y. Ozawa, and K. Eguchi, Catal. Today **59**, 69 (2000).
[4] G. J. Li, X. H. Zhang, and S. Kawi, Sens. Actuators B **60**, 64 (1999).
[5] M. Gaidi, B. Chenevier, and M. Labeau, Sens. Actuators B **62**, 43 (2000).
[6] A. Cabot, J. Arbiol, J. R. Morante, U. Weimar, N. Bârsan, and W. Göpel, Sens. Actuators B **70**, 87 (2000).
[7] C. Dekker, Phys. Today **52**, 22 (1999).
[8] Z. W. Pan, Z. R. Dai, and Z. L. Wang, Science **291**, 1947 (2001).
[9] J. Arbiol, R. Díaz, A. Cirera, F. Peiró, A. Cornet, J. R. Morante, F. Sanz, C. Mira, J. J. Delgado, G. Blanco and J. J. Calvino, Inst. Phys. Conf. Ser. (accepted for publication).
[10] S. Bernal, F. J. Botana, J. J. Calvino, C. López, J. A. Pérez-Omil, and J. M. Rodríguez-Izquierdo, J. Chem. Soc., Faraday Trans. **92**, 2799 (1996).
[11] J. A. Pérez-Omil, Ph. D. thesis, Universidad de Cádiz, Cádiz, Spain, 1994.
[12] P. Stadelmann, Ultramicroscopy **21**, 131 (1987).